

Air-Purging Configurations for Optical Pyrometers in Gas Turbines

A Major Project Report

Submitted to the Rajasthan Technical University
in partial fulfillment of requirements for the award of
degree

Bachelor of Technology

in

Mechanical Engineering

by

Mehul Purbia

19etcme007

Sohan Singh Sisodiya

19etcme010



**DEPARTMENT OF MECHANICAL ENGINEERING
TECHNO INDIA NJR INSTITUTE OF TECHNOLOGY
UDAIPUR, RAJASTHAN**

March 2023

**DEPARTMENT OF MECHANICAL ENGINEERING
TECHNO INDIA NJR INSTITUTE OF TECHNOLOGY
UDAIPUR, RAJASTHAN**

2022 - 23



CERTIFICATE

This is to certify that the report entitled **Air-Purging Configurations for Optical Pyrometers in Gas Turbines** sub-mitted by **Mehul Purbia** (19etcme007) & **Sohan Singh Sisodiya** (19etcme010), to Department of Mechanical Engineering in partial fulfillment of the B.Tech. degree in Mechanical Engineering is a bonafide record of the seminar work carried out by him under our guidance and supervision. This report in any form has not been submitted to any other University or Institute for any purpose.

Mr.AbhishekSharma
(Project Guide)
Assistant Professor
Dept. of ME
Techno India NJR
Institute of Technology
Udaipur, Rajasthan



Accurate Sensing Technologies

We measure temperature accurately in extreme conditions

AST/TRA/UDR/10/2022

03.10.2022

TO WHOMSOEVER IT MAY CONCERN

This is to certify that **MR. MEHUL PURBIA**, student of B.Tech. (Mechanical Engineering) from Techno India NJR Institute of Technology, Udaipur is working in **Accurate Sensing Technologies Pvt. Ltd.** as an intern since 03rd Oct 2022.

FOR ACCURATE SENSING TECHNOLOGIES PVT. LTD.

AUTHORISED SIGNATORY.

Accurate Sensing Technologies Pvt. Ltd

New Building, First Floor,
188 A, B-169 (Part), B-188 (A), Road No. - 5
Mewar Industrial Area, Udaipur (Rajasthan) - 313003
Phone : +91-294-3507736
Email : sales@accuratesensors.com
Web : www.accuratesensors.com

GSTIN No. : 08AAHCA9632N1Z4

DECLARATION

I **Mehul Purbia** hereby declare that the major project report **Air-Purging Configurations for Optical Pyrometers in Gas Turbines** , submitted for partial fulfillment of the requirements for the award of degree of Bachelor of Technology of the Rajasthan Technical University, Kota, Rajasthan is a bonafide work done by me under supervision of Mr.Abhishek Sharma

This submission represents my ideas in my own words and where ideas or words of others have been included, I have adequately and accurately cited and referenced the original sources.

I also declare that I have adhered to ethics of academic honesty and integrity and have not misrepresented or fabricated any data or idea or fact or source in my submission. I understand that any violation of the above will be a cause for disciplinary action by the institute and/or the University and can also evoke penal action from the sources which have thus not been properly cited or from whom proper permission has not been obtained. This report has not been previously formed the basis for the award of any degree, diploma or similar title of any other University.

Udaipur
25-03-2023

Mehul Purbia
Sohan Singh Sisodiya

Abstract

Optical pyrometers that operate in gas turbine aeroengines are exposed to contaminate particulates from the atmosphere of the operating environment, which can deposit on the instrument's lens and thus foul the system's optics. This particle deposition process results in the attenuation of the thermal radiation signal, from the pyrometer's measurement target, due to transmission losses through the layer of deposits on the lens. A purge air system is therefore employed to minimize the level of optical contamination. This article outlines the generic air- purging configurations and highlights their operation through providing both flow field and particle trajectory analyses via computational fluid dynamics (CFD) in order to provide an evaluation of their operating performance.

Acknowledgement

I take this opportunity to express my deepest sense of gratitude and sincere thanks to everyone who helped me to complete this work successfully. I express my sincere thanks to **Mr. Abhishek Sharma**, Head of Department, Mechanical Engineering, Techno India NJR Institute of Technology Udaipur for providing me with all the necessary facilities and support.

I would like to place on record my sincere gratitude to my project guide Mr. Abhishek Sharma, Assistant Professor, Mechanical Engineering, Techno India NJR Institute of Technology for the guidance and mentorship throughout the course.

Finally I thank my family, and friends who contributed to the successful fulfilment of this project work.

Mehul Purbia
Sohan Singh Sisodiya

Contents

Abstract	i
Acknowledgement	ii
1. Introduction	1
2. Sources of Contamination	3
3. Generic Purge Air Configuration	5
4. Air Curtain Configuration	6
5. Air Scrubbing Configuration	7
6. Still Tube Configuration	8
7. Numerical Modelling of the Purge System	9
8. Modeling Setup	10
9. Analysis of Flow Fields	12
10. Analysis of Particle Behavior	17
11. 3D Design of Purging Unit	21
11.1. Solidworks	21
12. Conclusion	23
13. Reference.	24

List of Figures

1.1. Air-Purging Configurations for Optical Pyrometers in Gas Turbine.	2
3.1. Fundamental purge design.	5
4.1. Air curtain configuration.	6
5.1. Air scrubbing configuration.	7
6.1. Still tube configuration.	8
8.1. Mesh for air scrubbing configuration.	11
9.1. Purge air pathlines for the air curtain configuration.	12
9.2. Purge air pathlines for the air scrubbing configuration.	12
9.3. Purge air pathlines for the still tube configuration.	12
9.4. Recirculations in the air curtain configuration.	13
9.5. Backflow in the air curtain configuration.	13
9.6. Recirculation in the air scrubbing configuration.	14
9.7. Purge flow into the still tube.	15
9.8. Recirculation in the still tube configuration.	15
9.9. Flow redirection in front of the still tube mouth.	16
10.1. Level of purge air deposition.	17
10.2. Purge air deposition in the air curtain configuration.	18
10.3. Purge air deposition in the still tube configuration.	19
10.4. Turbine chamber penetration in the still tube configuration.	19
10.5. Particla depostion configuration.	20
11.1. Design of Purging Unit	21
11.2. 3D section view of Purging Unit	22
11.3. 3D section view of Air Purge Component.	22

List of Tables

1. Boundary Condition for Numerical solutions	11
---	----

Chapter 1

Introduction

Optical pyrometry provides an effective means of direct temperature measurement of the turbine blades in gas turbine aeroengines.

However, the greatest concern with the in-service use of pyrometry is the issue of fouling, since the device's lens is exposed to the turbine environment.

The level of optical contamination can be minimized by incorporating a purge air system into the pyrometer design, whereby an air flow is sent down the pyrometer's sight tube to prevent particles in the turbine gas stream from coming in contact with the lens and therefore prevent the associated buildup of contaminants on its surface.

This article provides a review and evaluation of the basic purge air designs applicable to the problem of particulate contamination of pyrometer lenses.

Optical pyrometry is a noncontact method of surface temperature measurement that does not perturb the surface of the target material or surrounding medium. The technique is based on determining the temperature of an object by a measurement of the thermal radiation that is emitted from the object's surface. The device operates by collecting thermal radiation from a defined surface area, which is optically transferred to a detector, to produce an electrical signal proportional to the surface's radiant power. The optical pyrometers that are installed in gas turbine aeroengines provide direct temperature measurements of the turbine blades, with the resulting data being the primary input for providing a realistic assessment of the components' operating history and associated life usage

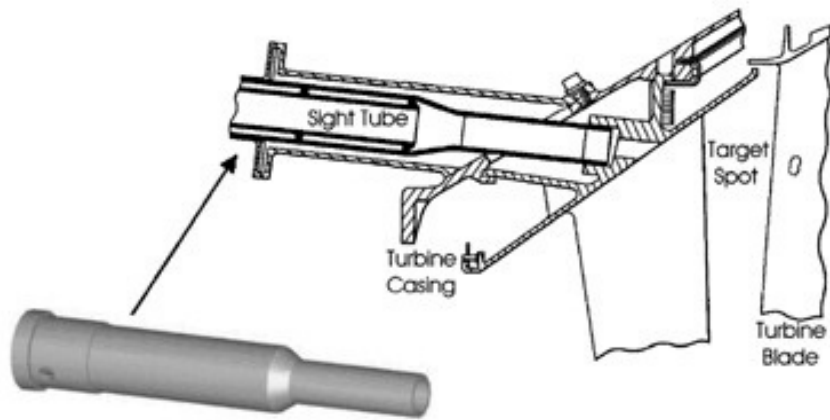


Figure 1.1: Air-Purging Configurations for Optical Pyrometers in Gas Turbines

The function of the sight tube assembly housing the pyrometer lens is to define the target spot and collect the emitted thermal radiation from the blades. However, this means that the pyrometer is open to the particle-laden gas stream of the turbine, and unfortunately the target on the turbine blade may become obscured due to particle deposition on the pyrometer lens.

Chapter 2

Sources of Contamination

There are only two sources of lens fouling within any pyrometer purge air system (Kerr and Ivey 2001). The first and most obvious is gas stream particles in the turbine chamber that enter through the sighting aperture of the sight tube.

It is this source of contamination, termed turbine chamber penetration, that the purge air system is employed to minimize, if not prevent. The operating mechanism of the purge system is to provide and maintain a positive pressure through the sight tube to prevent particulates in the turbine gas stream from penetrating the sight tube and reaching the lens.

Such penetrating particles typically have high inertia and thus the purge airflow must be adequate to redirect these contaminants back around and down the sight tube to re-enter the turbine chamber.

The most significant particulate matter in the turbine gas stream is the suspended particulates that result from the combustion process, with soot being the major constituent. Of course, there are many other particles present such as those that have been ingested by the engine, for example sand, and particles from the engine itself through erosion of components, such as protective coatings on the blades.

The other contributing factor to lens fouling, more subtle yet just as significant, is the fact that the source of purge air is bled from the compressor, which means that particles are present in the purge airflow itself. Thus, in certain designs the purge air can actually be attributed to the cause of lens fouling instead than minimizing deposition as was intended. This second source of contamination, termed purge air deposition, whereby particles from the purge air can deposit, is sometimes easily overlooked in some systems.

Compressor bleed air is used as the supply for the pyrometer purge system, and it is usually particle-laden with particulates that originate from the surrounding atmosphere ingested by the engine.

ginate from the surrounding atmosphere ingested by the engine.

A simple solution would be to remove these particles in the purge air through the use of a filter; however, such items are not favored due to maintenance issues, weight, and the fact that this is another component that must be added to the aeroengine together with the subsequent ramifications that may then emerge with its installation and maintenance.

Chapter 3

Generic Purge Air Configuration

The design concept for pyrometer purge air systems is to flow purge air down the elongated cylindrical sight tube that houses the lens. The action of the out-flowing purge air serves to stop most particles from flowing up through the sighting aperture and contacting the lens.

In general, the sight tube assembly consists of the lens housing, basically a tube that holds the lens in position, and a purge sleeve, which is another tube that fits in front of the lens housing and has a number of purge inlets for the introduction of the purge air, as illustrated in Figure 3.1. It should be noted that the purge inlets can be of any desired number sufficient to provide an adequate volume of purge flow and are generally circular in shape.

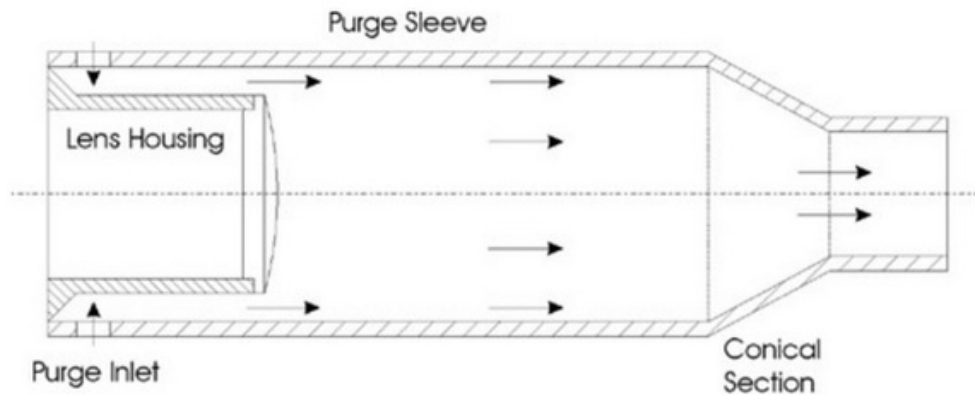


Figure 3.1: Fundamental purge design.

The purge sleeve consists of both cylindrical and conical sections that define a funnel-shape.

The resulting converging profile of the purge sleeve means that it functions as a nozzle so that the velocity of the purge airflow increases through the conical section in order to minimize any backflow within the sight tube that would otherwise draw particles in from the turbine chamber.

Chapter 4

Air Curtain Configuration

The design concept for the air curtain configuration, shown in Figure 4.1, is to provide an airflow in front of the lens, thus establishing a barrier that prevents any contaminants from entering the sight tube.

However, two disadvantages do emerge from this approach, namely particles may become trapped and then accumulate in the dead air zone between the lens and air curtain (Hayden et al. 1988). Secondly, there is no mechanism for removing any particles that may settle on the surface of the lens after the aeroengine shuts down, excluding of course cleaning during routine maintenance (Kerr and Ivey 2001).

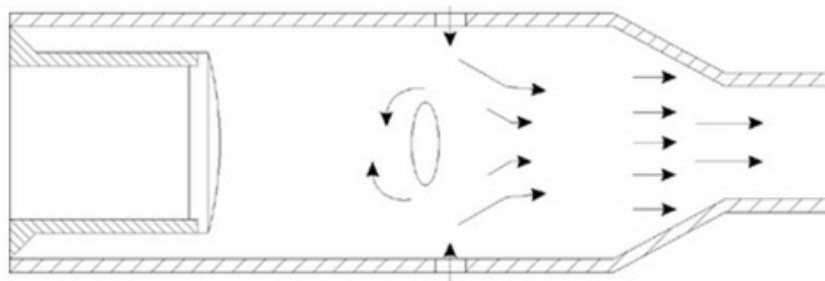


Figure 4.1: Air curtain configuration.

Chapter 5

Air Scrubbing Configuration

The air scrubbing approach utilizes the layer attachment or Coanda effect, whereby the purge airflow is directed over the lens surface so as to form a barrier to prevent any particulates penetrating the sight tube from coming into contact with the lens.

As the purge air flows over the lens it tends to scrub across its surface (Figure 5.1) and any particles on the lens will be re-entrained (Berenblut and Masom 1982; Hayden et al. 1988; MacKay 1990). The purge must be controlled so as to maintain an adequate flow velocity to insure that any particles that are removed from the lens remain entrained and are carried outwardly away from the lens.

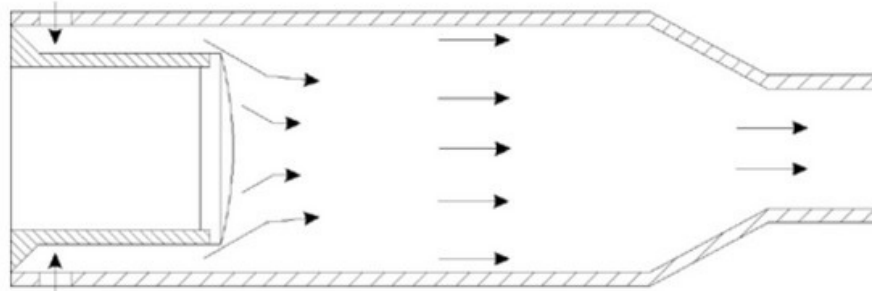


Figure 5.1: Air scrubbing configuration.

An important advantage of this generic configuration is that the scrubbing action permits the removal of ignition phase deposits that may form during engine start-up (Berenblut and Masom 1982). Also any particles that deposit as the aeroengine shuts down, due to gravitational settling for example, are then removed when the purge system begins to operate with engine start-up.

However, Hayden et al. (1998) acknowledged two principal disadvantages with the scrubbing approach: first, any particles in the purge air itself are brought to the lens, thus increasing the likelihood of deposition; and second, although the scrubbing action can remove large particles the technique experiences difficulty in removing submicron particles or large sticky particles already deposited

Chapter 6

Still Tube Configuration

The design concept for the still tube configuration is the same as the air curtain, i.e., to provide an airflow barrier in front of the lens.

However, this barrier of purge air is formed with the addition of a still tube extension in front of the lens, as presented in Figure 6.1. The still tube has the function of establishing a still region in front of the lens to prevent any contaminants, even those in the purge air itself, from depositing on the lens (Kerr and Ivey 2001).

The major disadvantage with this configuration is that there is no mechanism for removing any particles that may settle on the surface of the lens after the aeroengine shuts down, except manual cleaning conducted through routine maintenance.

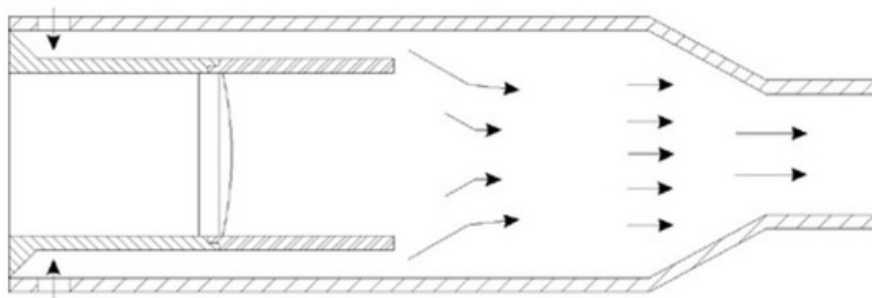


Figure 6.1: Still tube configuration.

Chapter 7

Numerical Modelling of the Purge System

Analysis of the three generic purging configurations (air curtain/air scrubbing/still tube) was conducted using computational fluid dynamics (CFD) to provide not only a deeper insight and understanding of each purging mechanism but also a performance evaluation. Solutions were acquired for the purging systems at the steady-state pressure operating condition, termed engine cruise, in order to discover the important flow features that develop within each of the designs.

The primary features to identify within the study of purge system airflows are any recirculations within the sight tube that may draw in contaminants or otherwise enhance particle deposition onto the pyrometer lens.

In addition to particle penetration from the turbine chamber up into the pyrometer sighting tube, particles were also injected into the purge flow to study deposition from the purge air itself.

Chapter 8

Modeling Setup

The solver chosen for the numerical study was FLUENT 5, which is a commercially available finite volume code produced by Fluent Incorporated (Fluent 1998). The GAMBIT program, which is a part of the FLUENT package, was the preprocessor used for geometry modeling and mesh generation for all of the grids produced in this study.

For modeling purposes, all three configurations share the same relative dimensions contained within an overall sight tube length of 160 mm. The purge air for each configuration is fed from a plenum surrounding the purge sleeve through a row of four inlets which are offset by an angle of 90° , with each inlet being circular in shape and having a diameter of 5 mm.

Through using GAMBIT, the three purge air system volumes were meshed using unstructured tetrahedral grids. The major motivation for using unstructured grids employing tetrahedral cells was the reduced mesh generation time.

Since CFD solutions require the use of finite grid spacings, the meshes must be generated in such a way that they correctly resolve the flow phenomenon of greatest importance without negatively affecting the accuracy of the solution or exceeding the computational resources available. Thus, a solution must be shown to be insensitive to the spacing of the grid to demonstrate that adequate mesh resolution has been used. Therefore, mesh independence tests were conducted whereby a series of grids with significantly differing resolutions were run until an acceptable balance of accuracy and computational complexity was achieved. For the models in this study, an example of which is illustrated in Figure 8.1, the resultant meshes contained in the region of 470,000 to 500,000 cells.

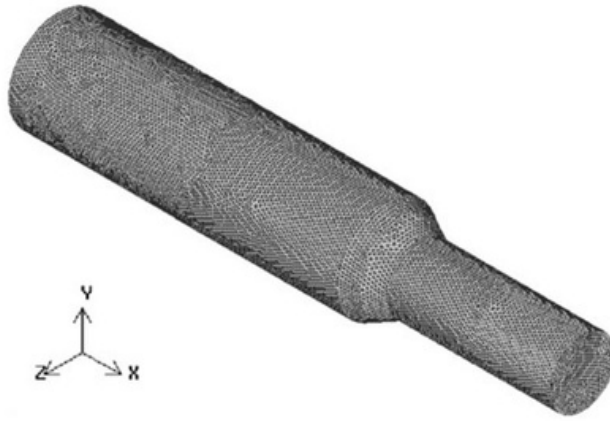


Figure 8.1: Mesh for air scrubbing configuration.

For the flow specification, a set of gas turbine representative boundary conditions were chosen for the numerical simulations with the purging systems operating under the steady-state conditions of engine cruise, as specified in Table 1. Within FLUENT, several test runs of the models were conducted in order to find the appropriate numerical schemes and settings to use, thus facilitating the constraints of computational cost versus accuracy.

Table 1
Boundary conditions for numerical simulations

	Pressure (kPa)	Temperature (K)
Purge inlets	900	580
Purge outlet	620	1125

The 3D, steady-state, segregated solver was found to be appropriate together with the SIMPLE method for pressure-velocity coupling. Since cyclonic swirls develop within the designs, the renormalization-group (RNG) k-e turbulence model provided the best balance in terms of run time, with a turbulence intensity of 10% and associated length scale of 0.1 mm. This solution strategy was validated experimentally through employing Laser Doppler Anemometry with a full-scale model of an actual inflight pyrometer purge system (Kerr 2002).

Chapter 9

Analysis of Flow Fields

The essence of a purge air system is to maintain a positive flow through the sight tube to prevent combustion gases with suspended particles from entering the pyrometer and contaminating the lens; Figures 7–9 show this positive purge flow for each of the three configurations.

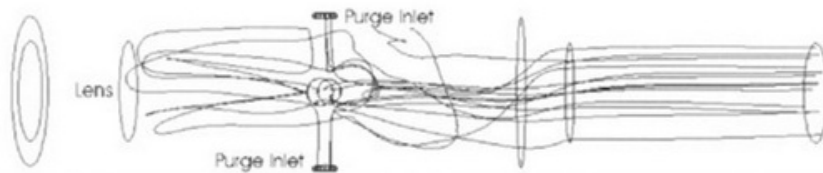


Figure 9.1: Purge air pathlines for the air curtain configuration.

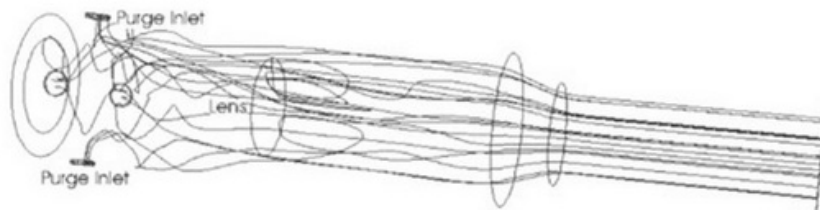


Figure 9.2: Purge air pathlines for the air scrubbing configuration.

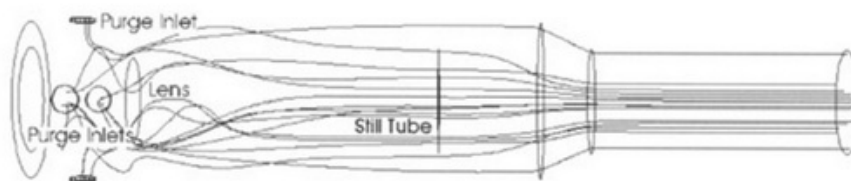


Figure 9.3: Purge air pathlines for the still tube configuration.

Consider first the air curtain purging system (Figures 3 and 7); although this design does produce a positive purge flow out through the sight tube, analysis of the purge air velocity vectors shows that there are in fact significant recirculations within the sight tube as illustrated in Figure 9.4 (significant is defined as large recirculations within the purge system that result in the establishment of a negative flow toward the pyrometer).

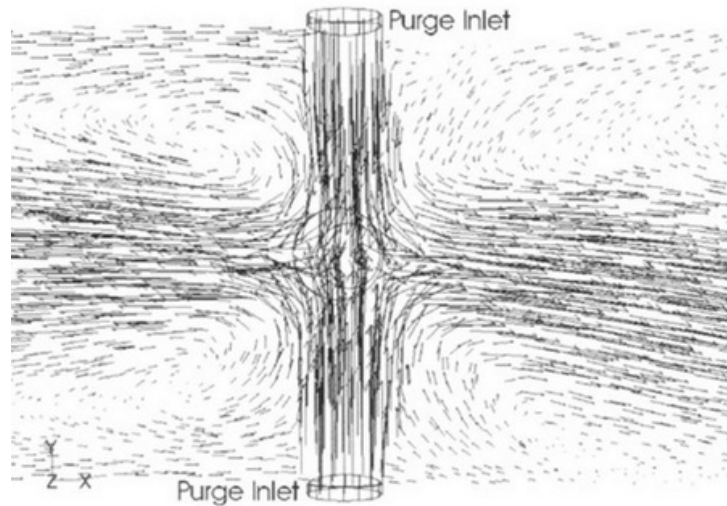


Figure 9.4: Recirculations in the air curtain configuration.

This not only results in an inefficient use of the purge airflow but leads to the formation of a backflow which develops when the purge air enters the inlets and the inlet jets mix. The development of this backflow (Figure 9.5) results in a major proportion of the purge air coming in contact with the pyrometer lens; should there be any particulates in the purge air then this backflow mechanism will greatly enhance the level of purge air deposition.

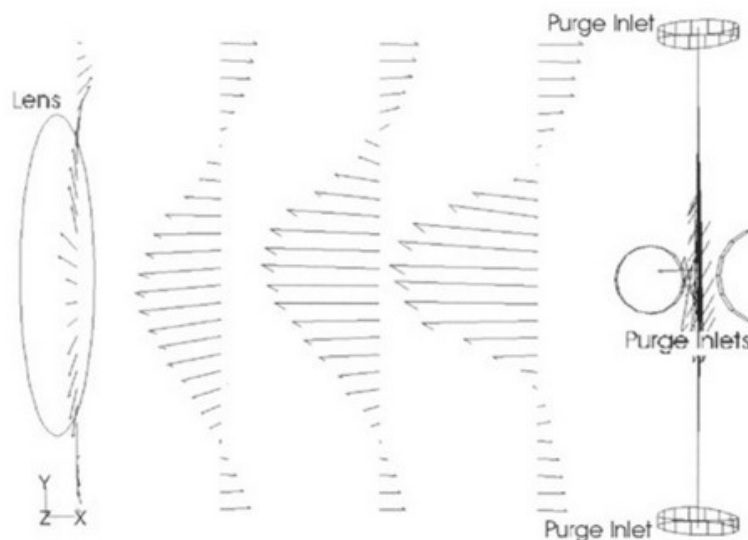


Figure 9.5: Backflow in the air curtain configuration.

For the air scrubbing purging system (Figures 4 and 8), it can be seen that this configuration will produce a more effective purge flow, i.e., a purge flow that results in a lower level of lens fouling, through the sight tube compared to the air curtain system. However, there are a number of pathlines that swirl in front of the lens. Upon closer inspection, it appears that instead of the purge air scrubbing across the lens there is a negative recirculation, depicted in Figure 9.6, as the purge sweeps around the lens, analogous to the flow situation of a backward-facing step.

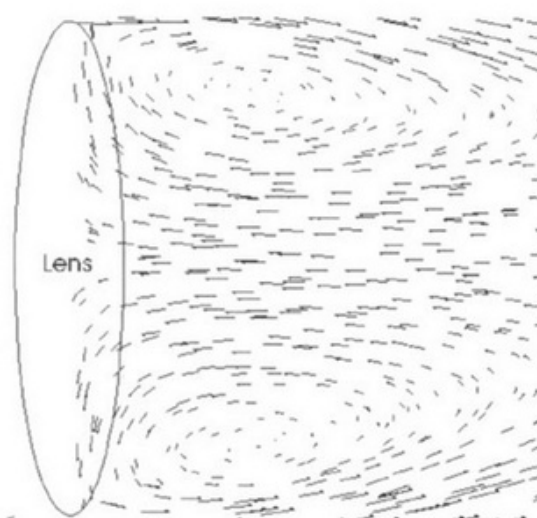


Figure 9.6: Recirculation in the air scrubbing configuration

This flow feature actually presents the fact that rather than developing a scrubbing action across the lens with the advantage of re-entraining any particles on the lens, such as the removal of ignition phase deposits or gravitationally settled particulates, the purge airflow actually enhances the buildup of deposits onto the lens.

Finally, consider the analysis of the flow field for the still tube purging system. Figure depicts the airflow pathlines maintaining the positive flow through the sight tube; however, Figure 9.7 illustrates that some of these pathlines may flow around the mouth of the still tube, which protects the pyrometer lens, and down its length.

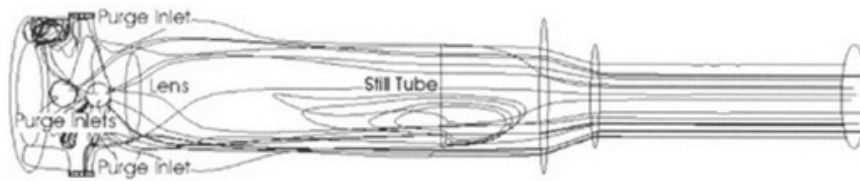


Figure 9.7: Purge flow into the still tube.

Analysis of the velocity vectors (Figure 9.8), shows that there is significant swirl or recirculation in front of the still tube mouth. Although Figure 14 only shows the swirl effect in a 2D cross-section, this recirculation is of course a 3D circumferential effect. The swirl that develops can be seen to converge a distance in front of the still tube mouth where a portion of the purge air undergoes a 180 ° direction change as it sweeps around from the annular passageway between the purge sleeve and outer wall of the still tube.

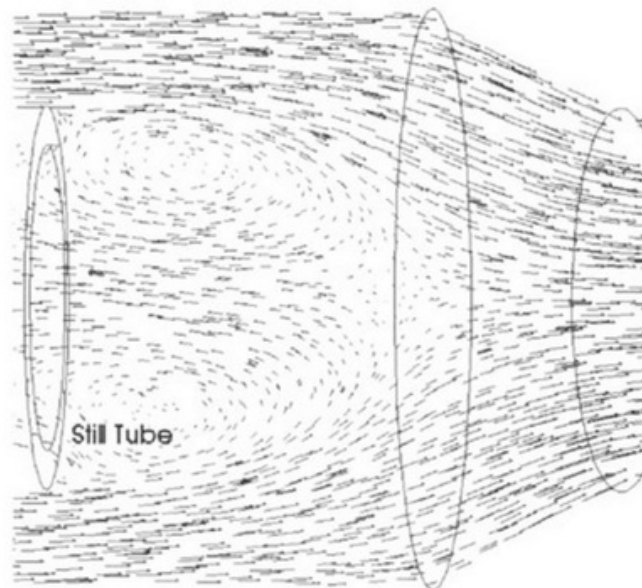


Figure 9.8: Recirculation in the still tube configuration

This redirection of airflow is presented in Figure 9.9. The danger with establishing this type of flow structure within the purge system is that it can draw contaminants through and down into the still tube, and once this airflow penetrates the core of the still tube it can then set up a highly cyclonic swirling flow. This means that any contaminants drawn into the still tube will eventually deposit onto the lens, resulting in lens fouling.

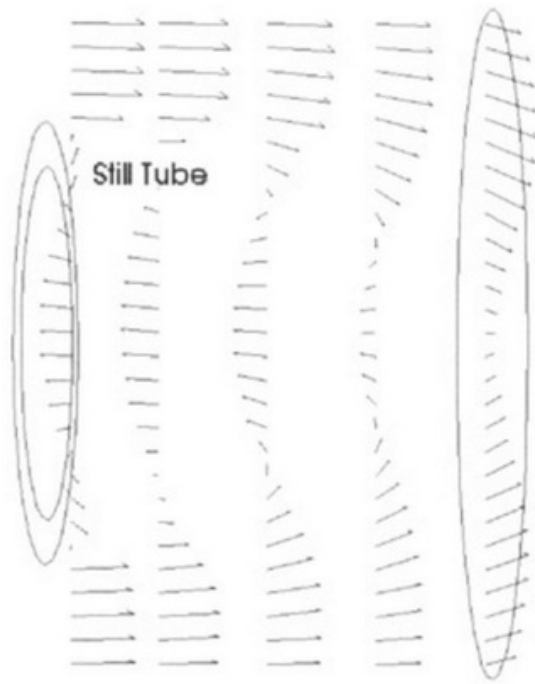


Figure 9.9: Flow redirection in front of the still tube mouth

Chapter 10

Analysis of Particle Behavior

Using FLUENT's built-in particle-tracking capabilities, particles were injected into the purge airflow to determine the level of particle deposition onto the surface of the pyrometer lens due to both purge air deposition and turbine chamber penetration. The level of deposition on the lens was evaluated in terms of the percentage particle deposition as defined by

$$\begin{aligned} &\text{Percentage Particle Deposition} \\ &= \frac{\text{Particles deposited on lens}}{\text{Particles injected into purge}} \times 100. \quad [1] \end{aligned}$$

Consider first the level of fouling due to contaminant particles in the purge air. An analysis of the percentage particle deposition versus particle diameter was conducted, through CFD modeling, for all three purge configurations, the results of which are presented in Figure 10.1.

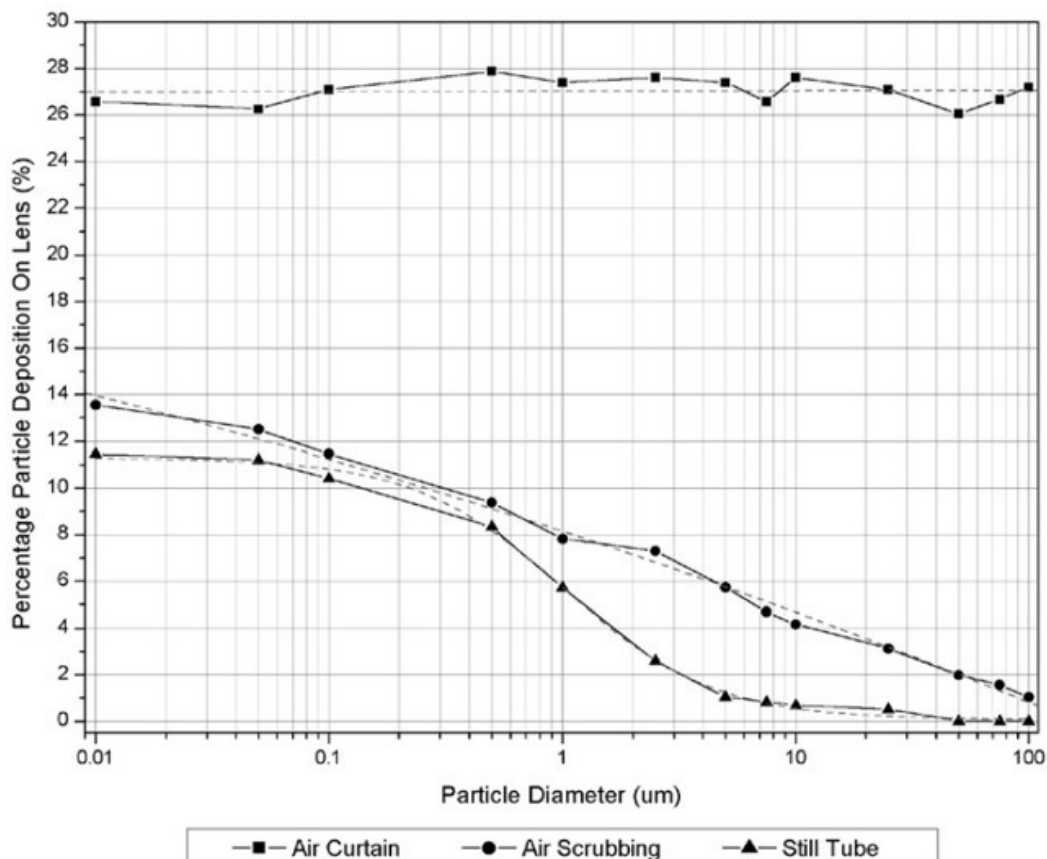


Figure 10.1 Level of purge air deposition.

The air curtain system shows a constant level of fouling, averaging at 27%, since a fixed portion of the particulates injected into the purge air will follow the backflow mechanism to impact upon the lens (Figure 10.2).

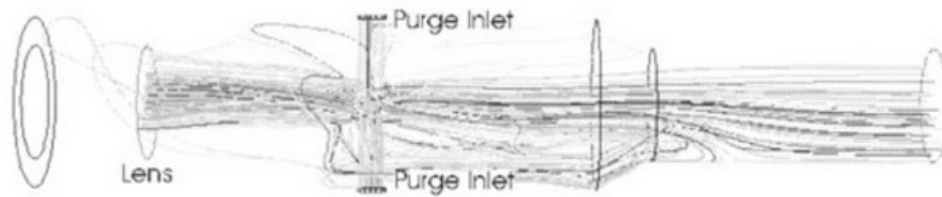


Figure 10.2: Purge air deposition in the air curtain configuration.

For the air scrubbing design, there are essentially three regions to the level of purge air deposition onto the pyrometer lens. First, for particles having a diameter smaller than $0.01 \mu\text{m}$ there is a constant level of deposition of approximately 13.5%. This is due to the fact that these smaller particles have a tendency to follow the airflow and therefore a fixed portion will become entrained by the negative recirculation in front of the lens. Secondly, there is a transition region between $0.01\text{--}100\mu\text{m}$ whereby the number of particles depositing on the lens decreases linearly with increasing particle diameter. This transition region is described by the function:

$$y = 8.147 - 3.282x - 0.190x^2 \quad (R^2 = 0.995) \quad [2]$$

Thirdly, for particles greater than $100 \mu\text{m}$ there is negligible purge air deposition since such particulates have high inertia and thus do not swirl around in front of the lens.

Analysis of the still tube configuration shows essentially the same three regions that have a contribution to purge air deposition as with the air scrubbing system. For particles less than $0.01 \mu\text{m}$ there is a constant level of deposition of approximately 11.5%. These smaller particles remain entrained with the purge airflow, and therefore a fixed portion will become captured by the swirl at the still tube mouth such that they then flow down the still tube to impact the lens. There is also a transition region between $0.01\text{--}50 \mu\text{m}$ whereby the number of particles drawn into the still tube, due to the swirling pattern at the still tube mouth, and depositing on the lens decreases with increasing particle diameter. The transition region of the still tube system is described by the sigmoid:

$$y = \frac{11.286 - 0.060}{1 + (x/1.019)^{1.347}} \quad (R^2 = 0.994). \quad [3]$$

Finally, particles greater than $50\ \mu\text{m}$ have such a high inertia that they do not swirl around into the still tube and therefore have a negligible effect on lens fouling. Figure 10.3 depicts the particle tracks for both a large particle ($100\ \mu\text{m}$), which does not deposit, and a small particle ($0.1\ \mu\text{m}$), which is captured by the swirl pattern at the mouth of the still tube, resulting in deposition onto the lens. Finally, particles greater than $50\ \mu\text{m}$ have such a high inertia that they do not swirl around into the still tube and therefore have a negligible effect on lens fouling. Figure 18 depicts the particle tracks for both a large particle ($100\ \mu\text{m}$), which does not deposit, and a small particle ($0.1\ \mu\text{m}$), which is captured by the swirl pattern at the mouth of the still tube, resulting in deposition onto the lens.

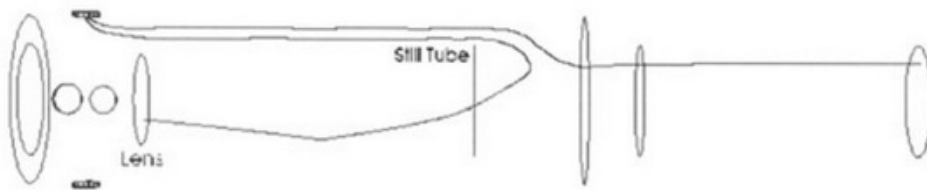


Figure 10.3: Purge air deposition in the still tube configuration.

Consider next the level of optical contamination due to turbine gas path particles penetrating the pyrometer sight tube; ideally the purge airflow should redirect any particulates back into the turbine chamber as depicted in Figure 10.4. However, certain particles with a high enough inertia can shoot directly up through the sight tube and into the still tube to impact with the lens (Figure 10.4).

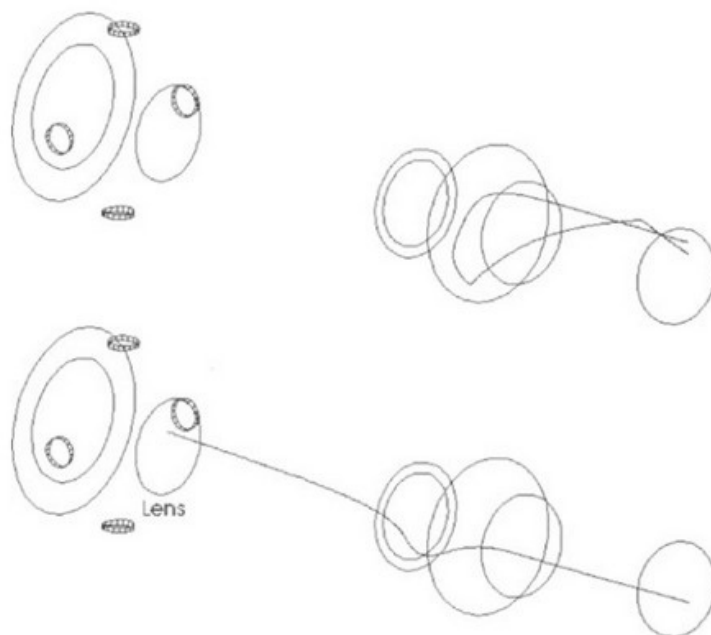


Figure 10.4: Turbine chamber penetration in the still tube configuration.

Analysis of the percentage particle deposition versus particle diameter, with an initial particle velocity of 100 m/s due to turbine chamber penetration was conducted at the steady-state operating condition and these results are presented in Figure 10.5. This graph shows that there are essentially three regions that have a contribution to the problem of lens fouling for each of the purge air configurations. Firstly, for each system there is negligible deposition below a specific particle diameter. For instance, contaminants penetrating the air curtain configuration with an initial velocity of 100 m/s and particles having a diameter less than 30 μm are completely redirected back out of the sight tube, since they do not have enough inertia to overcome the opposing purge airflow. For the air scrubbing and still tube configurations this minimum critical particle diameter is 80 μm and 75 μm , respectively. Secondly, there is a transition region through a range of particle diameters whereby the number of particles that have the ability to impact and thus deposit on the lens increases with increasing particle diameter. For the air curtain design, this transition region is linear and is expressed by the function.

$$y = -22.898 + 0.878x \quad (R^2 = 0.994). \quad [4]$$

For both the air scrubbing and still tube designs the transition region takes the form of a sigmoidal curve having the following functions:

$$\text{Air Scrubbing: } y = \frac{-100}{1 + e^{(x-97.946)/3.139}} \quad (R^2 = 0.995), \quad [5]$$

$$\text{Still Tube: } y = \frac{-100}{1 + e^{(x-90.933)/3.144}} \quad (R^2 = 0.998). \quad [6]$$

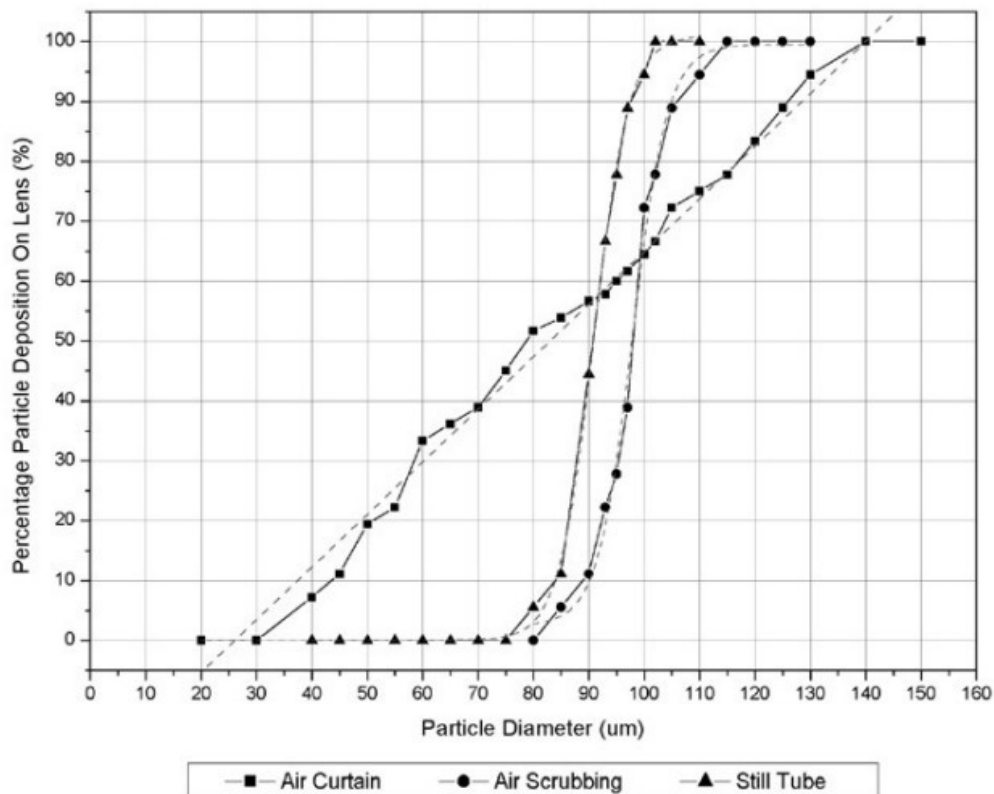


Figure 10.5 Particla depostion configuration.

Chapter 11

3D design of purging unit

Solidworks

SolidWorks is computer-aided design (CAD) software owned by Dassault Systèmes. It uses the principle of parametric design and generates three kinds of interconnected files: the part, the assembly, and the drawing. Therefore, any modification to one of these three files will be reflected in the other two.

SOLIDWORKS uses parametric design, which is why it's such an effective tool for designers and engineers. This means that the designer can see how changes will affect its neighboring components, or even the overall solution. For example, if the size of a single component is increased, this would affect the joint or hole it's attached to. This allows designers to spot and correct issues quickly and easily.

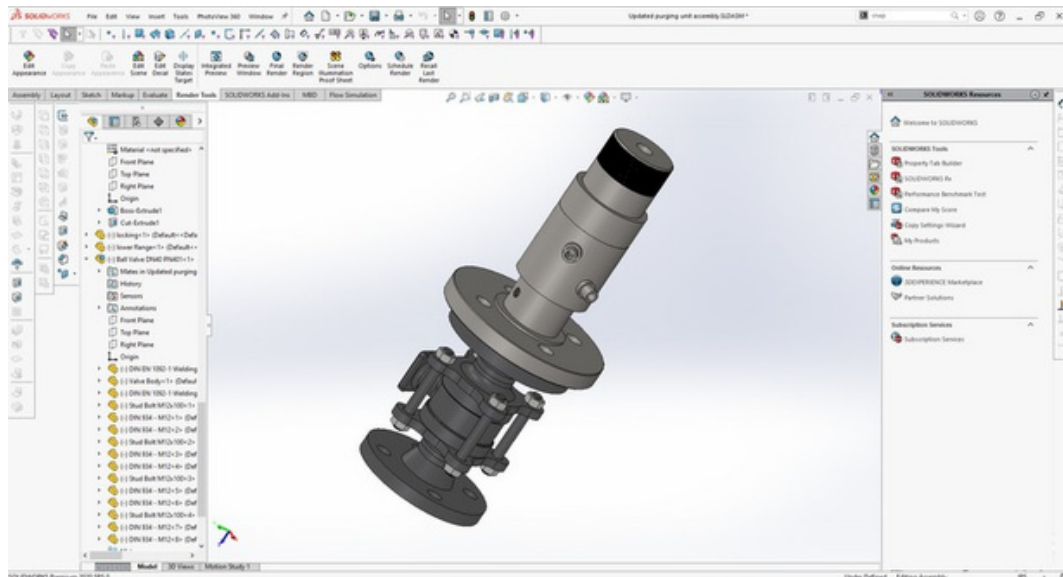


Figure 11.1 3D design of Purging unit

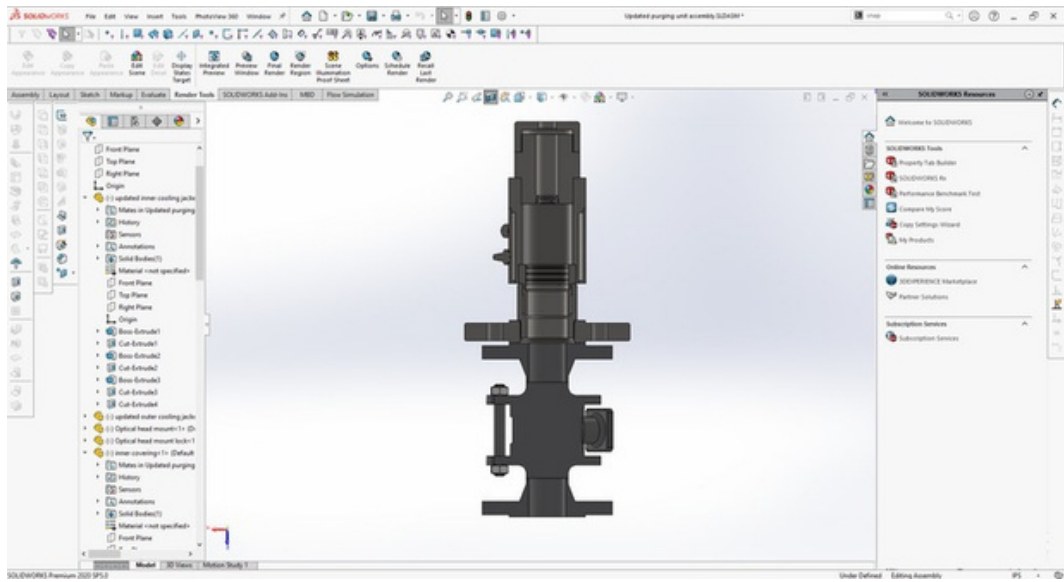


Figure 11.2 3D section view of Purging unit

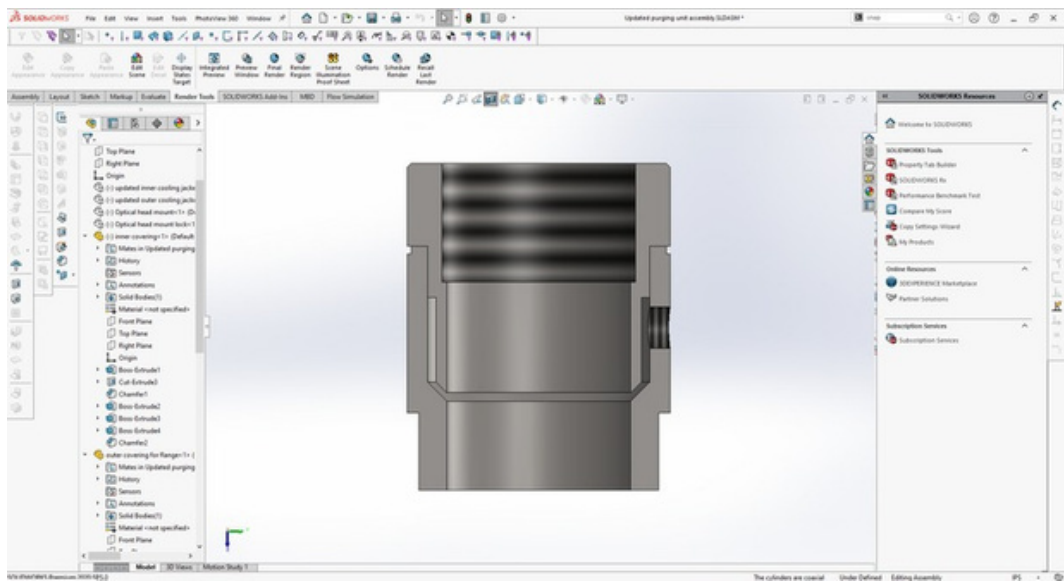


Figure 11.3 3D section view of Air purge component

Chapter 12

Conclusion

The task of the pyrometer purge air system is to keep the instrument's lens, clean, or at least to minimize the level optical fouling, and there are principally three generic purge designs that can be utilized, namely, the air curtain, air scrubbing, and still tube configurations.

The air scrubbing design operates by directing the purge airflow over the lens so as to scrub across its surface. However, from flow field analysis it was found that there was a negative recirculation that develops in front of the lens, and this flow feature actually enhances the buildup of deposits onto the lens. This configuration had a purge air deposition profile of 13.5% at 0.01 μm , down to 0% at 100 μm . In terms of particle penetration up the sight tube, the air scrubbing design was capable of completely redirecting particles with a diameter up to 80 μm and an initial velocity of 100 m/s.

The still tube configuration, as its name implies, employs a still tube extension in front of the lens in order to establish a still region of air that will prevent any contaminants, even those in the purge air itself, from depositing on the pyrometer lens.

The predominant flow feature within this system was the significant recirculation, or swirl, of the purge air in front of the still tube mouth. Once this swirl pattern is developed a subsequent negative flow is established into the core of the still tube. This motion will significantly increase the likelihood of contaminants coming in contact with the lens surface and depositing to result in optical fouling.

In making a comparison between each configuration, the air curtain design exhibited the highest level of particle deposition for both purge air deposition and turbine chamber penetration. It therefore had the worst operating characteristics and performance of all the three generic configurations. The air scrubbing system had the most effective barrier for preventing contaminants from penetrating the sight tube and depositing on the lens. Overall the still tube configuration offered the lowest level of purge air deposition and, with a comparable level of turbine chamber penetration to the air scrubbing design, presented the most effective pyrometer purge air configuration.

References

Barber, R. (1969). A Radiation Pyrometer Designed for In-Flight Measurement of Turbine Blade Temperatures, SAE 690432, National Air Transportation Meeting, New York, 21–24 April.

Berenblut, B. J., and Masom, R. A. (1982). Radiation Pyrometry for Gas Turbine Engines—An Introduction, *British J. Non-Destructive Testing* 24(5):268–269.

Fluent Incorporated (1998). *FLUENT 5 User's Guide*, Fluent Incorporated, Cavendish Court, Lebanon.

Hayden, T., Myhre, D., Pui, D. Y. H., Kuehn, T. H., and Tsai, C. J. (1988). Evaluating Lens Purge Systems for Optical Sensors on Turbine Engines, AIAA- 88- 3037, AIAA/ASME/SAE/ASEE 24th Joint Propulsion Conference, Boston, 11–13 July.

Kerr, C. I. V. (2002). Purge System Design for the Application of Optical Pyrometry in Aeroengines, EngD thesis, School of Engineering, Cranfield University, Cranfield, U.K.

Kerr, C. I., and Ivey, P. C. (2001). A Review of Purge Air Designs for Aeroengine Based Optical Pyrometers, ASME 2001-GT-0580, 46th ASME International Gas Turbine and Aeroengine Technical Congress, Exposition and Users Symposium, New Orleans, LA, 4–6 June.

Kerr, C. I., and Ivey, P. C. (2002). Particle Deposition on Optical Pyrometer Lenses: An Illustrative Case Study, *J. Aerosol Sci.* 33(11):1577–1588.

Kirby, P. J. (1986). Some Considerations Relating to Aero Engine Pyrometry, AGARD-CP-399, Advanced Instrumentation for Aero Engine Components, The Propulsion and Energetics Panel 67th Symposium, Philadelphia, 19–23 May.

MacKay, C. G. (1990). Temperature Measurement in Turbine Engines, AlliedSignal Inc., US Patent 4,934,137.